Voltage-activated Ca^{2+} channels and their role in the endocrine function of the pituitary gland in newborn and adult mice

Simon Sedej[1], Tetsuhiro Tsujimoto[2], Robert Zorec[3] and Marjan Rupnik[1]

[1] *European Neuroscience Institute Göttingen, Waldweg 33, 37073 Göttingen, Germany*
[2] *Department of Neurophysiology, University of Tokyo, Graduate School of Medicine, Tokyo 113-0033, Japan*
[3] *Laboratory of Neuroendocrinology – Molecular Cell Physiology, Institute of Pathophysiology, Medical School, University of Ljubljana, Zaloška 4, 1000 Ljubljana, Slovenia; Celica, Stegne 21, 1000 Ljubljana, Slovenia*

We have prepared fresh pituitary gland slices from adult and, for the first time, from newborn mice to assess modulation of secretory activity via voltage-activated Ca^{2+} channels (VACCs). Currents through VACCs and membrane capacitance have been measured with the whole-cell patch-clamp technique. Melanotrophs in newborns were significantly larger than in adults. In both newborn and adult melanotrophs activation of VACCs triggered exocytosis. All pharmacologically isolated VACC types contributed equally to the secretory activity. However, the relative proportion of VACCs differed between newborns and adults. In newborn cells L-type channels dominated and, in addition, an exclusive expression of a toxin-resistant R-type-like current was found. The expression of L-type VACCs was up-regulated by the increased oestrogen levels observed in females, and was even more emphasized in the cells of pregnant females and oestrogen-treated adult male mice. We suggest a general mechanism modulating endocrine secretion in the presence of oestrogen and particularly higher sensitivity to treatments with L-type channel blockers during high oestrogen physiological states.

(Resubmitted 18 December 2003; accepted after revision 8 January 2004; first published online 14 January 2004)
Corresponding author M. Rupnik: European Neuroscience Institute Göttingen, Waldweg 33, 37073 Göttingen, Germany. Email: mrupnik@gwdg.de

The melanotrophs from the intermediate lobe of the pituitary gland release pro-opiomelacortin (POMC)-derived peptide hormones (Mains & Eipper, 1979) in a Ca^{2+}-dependent manner (Douglas & Taraskevich, 1978). Ca^{2+} acts primarily through activation of VACCs (Douglas & Taraskevich, 1978; Douglas & Taraskevich, 1980), which triggers exocytosis. Adult melanotrophs express at least five different types of VACCs: the low voltage-activated (LVA) T-type and the high voltage-activated (HVA) Ca^{2+} channels including L-, N-, P-, and Q-type (Keja *et al.* 1991; Stack & Surprenant, 1991; Ciranna *et al.* 1996; Mansvelder & Kits, 2000). So far, a significant toxin-resistant R-type current has not been described in melanotrophs. All VACCs have been found to contribute equally to the secretory activity of cultured rat melanotrophs (Mansvelder & Kits, 2000).

Pronounced differences have been reported in relative densities of each VACC type in primary and clonal endocrine cells (Mansvelder *et al.* 1996; Mansvelder & Kits, 2000; Glassmeier *et al.* 2001; Cuchillo-Ibanez *et al.* 2002). Suggested sources for these differences have been interspecies differences (Cuchillo-Ibanez *et al.* 2002), recording temperature and charge carrier used (Mansvelder & Kits, 2000). Despite large variability, an apparent pattern from these reports has been that the fraction of the Ba^{2+} currents through N-type channels is around 30%. Fractions of L- and P/Q-types vary considerably, one or another being the dominant VACC (see Table 1). The tendency has been that the endocrine cells from adult females and young animals show larger L-type currents compared to cells from adult males.

In a number of glands, including the pituitary, hormones and neurotransmitters have been reported to regulate the expression of VACCs. Dopamine (Cote *et al.* 1982; Stack & Surprenant, 1991; Nussinovitch & Kleinhaus, 1992; Chronwall *et al.* 1995; Fass *et al.* 1999) and serotonin (Ciranna *et al.* 1996) inhibit the expression of VACCs in melanotrophs. Conversely, dopamine antagonists (Cherñavsky *et al.* 1993) and oestrogens (Heiman & Ben Jonathan, 1982) have been implicated in

 DOI: 10.1113.jphysiol.2003.058271

Table 1. The relative contribution of HVA currents in the different neuroendocrine systems

	% of HVA currents				Experimental data			
Reference	L	N	P/Q	R	sex	age/species/cell type	CC (mM)[a]	*T* [°C]
Albillos *et al.* 1993	15–20	30	50–55	—	—	Adult/bovine/chromaffin	2/10 Ba^{2+}	RT[d]
Gandia *et al.* 1993	29	41	55	—	—	Adult/bovine/chromaffin	10 Ba^{2+}	RT
Albillos *et al.* 1994	50	45	5	—	—	Adult/cat/chromaffin	10 Ba^{2+}	RT
Hernandez-Guijo *et al.* 1998	48	26	53–63	—	—	Adult/mouse/chromaffin	2/10 Ba^{2+}	RT
Gandia *et al.* 1995	48	31[b]	51[b]	—	—	Adult/rat/chromaffin	10 Ba^{2+}	RT
Mansvelder *et al.* 1996	35	26	31	—	M	Adult/rat/melanotroph	13 Ba^{2+}	RT
Ciranna *et al.* 1996	39	—	61	—	—	Juvenile/rat/melanotroph	2 Ca^{2+}	RT
Kitamura *et al.* 1997	85	22	94	—	—	Adult/pig/chromaffin	5/10 Ca^{2+}	RT
Gandia *et al.* 1998	25	21	60	—	F	Adult/human/chromaffin	10 Ba^{2+}	RT
Mansvelder & Kits, 2000	21	30	53	—	M	Adult/rat/melanotroph	5 Ba^{2+}	32–34
Glassmeier *et al.* 2001	49	—	40	24	F	Immortal line/rat/GH3	10 Ba^{2+}	RT
Present paper	45	28	17	14	M/F	NB[c]/mouse/melanotroph	10 Ba^{2+}	29–31
Present paper	15	23	50	4	M/F	Adult/mouse/melanotroph	10 Ba^{2+}	29–31
Present paper	42	26	20	14	M/F	NB/mouse/melanotroph	2 Ca^{2+}	29–31
Present paper	23	27	29	—	M/F	Adult/mouse/melanotroph	2 Ca^{2+}	29–31
Present paper	86	no data	no data	—	F	Pregnant/mouse/melanotroph	2 Ca^{2+}	29–31

[a]CC = charge carrier; [b]overlap in toxin sensitivities; [c]NB = newborn; [d]RT = room temperature.

the induction of expression of VACCs in anterior pituitary cells (Cherñavsky *et al.* 1993). Particularly the action of oestrogens indicates that additional sources of variability might be attributed to the sex and age of the animals tested. Our aim was to electrophysiologically characterize VACCs in the newborn and adult pituitary gland. For the first time we extended the slicing technique to a newborn mouse pituitary slice preparation. The present work also forms a foundation for the analysis of endocrine cells in the specific gene knockouts which die at birth. This novel approach enabled us to estimate the contribution of 17β-oestradiol on the sex- and age-dependent heterogeneity of the expression of different VACC types. In addition, we have tested the efficacy of the VACC in supporting endocrine function in the same experimental conditions.

Our data suggest a general physiological mechanism for augmentation of exocytosis in neuroendocrine cells by 17β-oestradiol-dependent up-regulation of voltage-activated L-type channels.

Methods

Fresh pituitary tissue slices

Electrophysiological experiments were performed on single melanotrophs within the intact clusters of the intermediate lobe of the pituitary gland. All mice (adult: 6–10 weeks old; newborn: P1–P2) were killed in a CO_2 atmosphere prior to decapitation. Animal work was performed according to the regulations of the State of Lower Saxony, Germany. The skull and brain were rapidly removed; the pituitary was then carefully dissected out and placed in an ice-cold external solution 1 (see Solutions) for approximately 2 min. The whole gland was then embedded in the 2.5% low-melting point agarose (Seaplaque GTG agarose, BMA, Walkersville, MD, USA) in 1 × phosphate-buffered saline (PBS) solution. The hardened agarose block was glued with cyanoacrylate (Super Glue, ND Industries, Troy, MI, USA) on to the sample plate of the vibrotome and covered with ice-cold external solution 2 (see Solutions). To preserve the gland morphology, 70–80 μm thick slices were sectioned on the vibrotome VT 1000 S (Leica, Nussloch, Germany) at 55–60 Hz and at 0.1 mm s^{-1}. Fresh slices were immediately transferred into an incubation beaker containing the oxygenated external solution 1 (see Solutions). Slices were kept at 32°C up to 8 h.

Solutions

The composition of external solution 1 was (mM): NaCl 125, KCl 2.5, NaH_2PO_4 1.25, sodium pyruvate 2, *myo*-inositol 3, ascorbic acid 0.5, glucose 10, $NaHCO_3$ 26, $MgCl_2$ 3, $CaCl_2$ 0.1, lactic acid 6. Low Ca^{2+} and high Mg^{2+} concentrations in the extracellular solution prevented spontaneous action potential firing. Pituitary glands were cut in external solution 2 containing (mM): KCl 2.5, NaH_2PO_4 1.25, sodium pyruvate 2, *myo*-inositol 3, ascorbic acid 0.5, sucrose 250, glucose 10, $NaHCO_3$ 26, $MgCl_2$ 3, $CaCl_2$ 0.1, lactic acid 6. The osmolality of this solution was 360 ± 10 mosmol kg^{-1}.

To isolate VACCs external solution 3 was used containing (mM): TEA-Cl 140, $MgCl_2$ 1.2, $BaCl_2$ 10 and Hepes 10; pH was adjusted to 7.3 with

TEA-OH. Tetrodotoxin (TTX, 1 μM) was added to block TTX-sensitive Na^+ currents. Capacitance measurements and measurements of Ca^{2+} currents were performed in external solution 4 composed of (mM): NaCl 125, KCl 2.5, NaH_2PO_4 1.25, sodium pyruvate 2, *myo*-inositol 3, ascorbic acid 0.5, glucose 10, $NaHCO_3$ 26, $MgCl_2$ 1, $CaCl_2$ 2, lactic acid 6. The osmolality of solutions 1, 3, 4 and the intracellular solution was 300 ± 10 mosmol kg^{-1}. External solutions 1, 2 and 4 were continuously bubbled with 95% O_2 and 5% CO_2 to enrich the oxygen content (pH 7.3).

The intracellular solution for current measurements was designed to isolate Ba^{2+} and Ca^{2+} currents and to block K^+ conductance (mM): CsCl 140, Hepes 10, $MgCl_2$ 2, TEA-Cl 20, Na_2ATP 2, EGTA 10; pH was adjusted to 7.2 with CsOH. The pipette solution for capacitance measurements differed only in EGTA concentration, which was 0.05 mM. All chemicals were supplied from Sigma (St Louis, MO, USA) unless otherwise indicated.

Ca^{2+} measurements

Intracellular Ca^{2+} concentration ($[Ca^{2+}]_i$) measurements were performed by using 0.5 mM fura-6F (Molecular Probes, Eugene, OR, USA), which was dialysed into the cytosol via a patch pipette. Fura-6F was excited at 380 nm with monochromatic light (Polychrome IV, TILL Photonics, Graefellfing, Germany; dichroic mirror 400 nm). The fluorescence intensity was measured at wavelengths longer than 420 nm by a photodiode (TILL Photonics). The filtered signal was recorded together with the traces of the voltage-clamp recordings. $[Ca^{2+}]_i$ was calculated as described by Carter & Ogden (1994). The equation used in the calculation is:

$$[Ca^{2+}]_i = K_d \frac{F - F_{min}}{F_{max} - F}$$

where K_d is the apparent dissociation constant for fura-6F (5.3 μM; Gee *et al.* 2000), F_{max} is the autofluorescence in a cell-attached configuration, F_{min} is fluorescence in a resting whole-cell recording and F is fluorescence during the voltage protocol.

Electrophysiology

The upright microscope Nikon Eclipse E600 FN (Nikon, Tokyo, Japan) was used for visualizing the cells with a 10 × DIC air objective (NA 0.3, WD 16 mm) and water immersion 60 × DIC objective (NA 1.0, WD 2 mm) with a mounted CCD camera (Cohu, San Diego, CA, USA). Intermediate lobe cells were easily distinguished from other cells as a narrow band engulfing the posterior pituitary (Fig. 1*A*). Seals were formed on identifiable

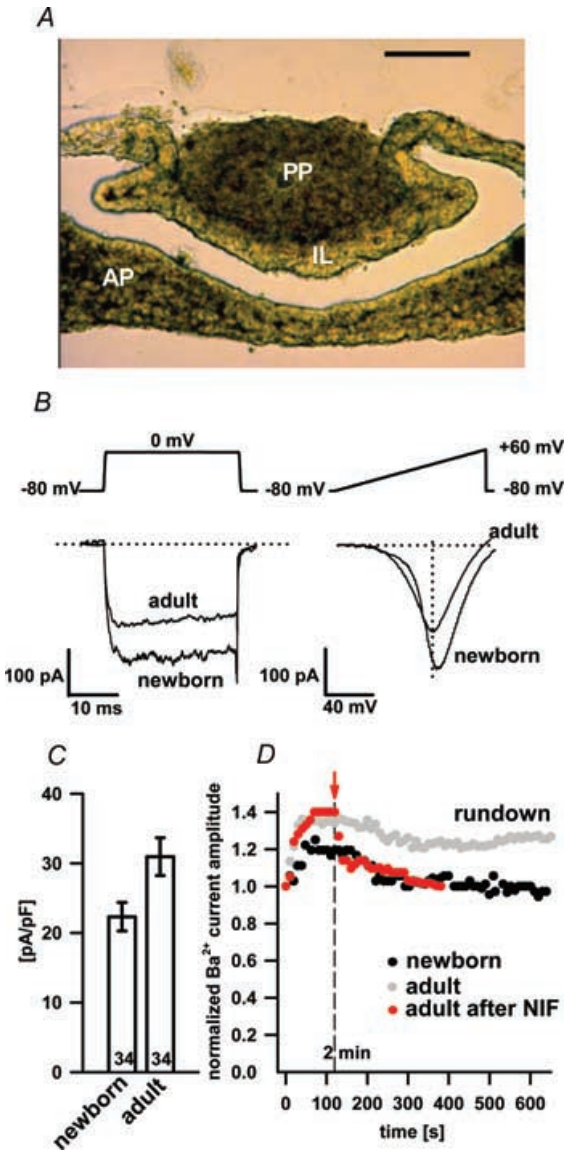

Figure 1. Newborn (P1) pituitary tissue slice (*A*), the separation of VACCs by pulse depolarization and voltage ramps (*B*), HVA peak Ba^{2+} current density (*C*) and washout of Ba^{2+} currents (*D*)
A, the newborn (P1) pituitary tissue slice (scale bar 100 μm; transmission photomicrography). The intermediate lobe (IL) is clearly distinguishable from the anterior (AP) and posterior part (PP) as a narrow band consisting of melanotrophs. *B*, representative traces of whole-cell Ba^{2+} currents evoked by 30 ms depolarization steps from −80 mV to 0 mV (left) and 300 ms voltage ramps from −80 mV to + 60 mV (right) in control conditions. Note that the peak amplitude of 30 ms depolarization traces corresponds to the peak amplitude of the HVA component obtained by the 300 ms voltage ramp. *C*, histogram of HVA peak Ba^{2+} current densities in adult and newborn melanotrophs. Numbers on bars represent the number of cells tested. *D*, the washout of Ba^{2+} currents in adult (open symbols) and newborn (filled symbols) melanotrophs during 10 min of dialysis and time dependence of nifedipine block (10 μM) of L-type Ba^{2+} currents in adult melanotrophs (red symbols). Nifedipine was applied 2 min after the whole-cell dialysis (see red bar).

cells by breaking the connective tissue envelope of a cluster using a gentle positive pressure. Stable recordings could be obtained between 1 and at least 8 h after slicing, similar to brain slices (Sakmann & Stuart, 1995). All electrophysiological experiments were performed at 29–31°C. Pituitary slices were held at the bottom of the recording chamber with parallel nylon strings stretched on a U-shaped platinum wire. During experiments the recording chamber was continuously superfused with heated solutions 3 or 4 at 1–2 ml min^{-1}. Pipettes were pulled using a puller (P-97, Sutter Instruments, Novato, CA, USA) from borosilicate glass capillaries (GC150F-15, WPI, Sarasota, FL, USA) and heat polished to obtain a pipette resistance of 2–4 MΩl in a KCl based solution. Whole-cell currents (Hamill *et al.* 1981) and capacitance changes were measured with a lock-in patch-clamp amplifier (SWAM IIC, Celica, Ljubljana, Slovenia; Zorec *et al.* 1991), low-pass filtered (3 kHz, –3 dB) and stored on a standard PC. We used WinWCP V3.2.6 software from J. Dempster (Strathclyde University, Glasgow) for pulse generation, data acquisition and basic analysis. Signal processing was done using Matlab (Mathworks, Novi, MI, USA) and figures were prepared in SigmaPlot (SPSS, Chicago, IL, USA). Cells were voltage clamped at −80 mV. The standard steady-state current–voltage analysis was performed using a family of 30 ms depolarization pulses in 10 mV steps from −80 mV to 60 mV. A set of five consecutive voltage ramps from −80 mV to +60 mV of 300 ms duration (voltage gradient 0.47 V s^{-1}) with a 1.5 s interval between sweeps was applied to separate the low from the high VACCs (Kocmur & Zorec, 1993). Averaged records were taken for analysis. Ba^{2+} and Ca^{2+} currents were leak subtracted. Secretory activity was triggered by a train of 50 depolarization pulses from −80 mV to +10 mV of 40 ms duration with 100 ms interval. Statistics are given as means ± S.E.M. The statistical significance of comparisons was assessed using Student's *t* test. One-way ANOVA was performed by using SigmaStat (SPSS) to determine whether differences between the various groups existed. ANOVA was tested by Tuckey's *post hoc* follow up test and the significance level was chosen at $P < 0.05$.

Pharmacology

Purified ω-conotoxin GVIA (GVIA), ω-conotoxin MVIIC (MVIIC), ω-agatoxin TK (TK) and SNX-482 were purchased from Alomone Laboratories (Jerusalem, Israel) and dissolved in distilled water to obtain stock solutions at concentrations of 100 μM, 10 μM, 1 μM and 1 μM, respectively. Toxins were kept in aliquots at −20°C and than applied manually to reach the final concentration in the recording chamber. Nifedipine (NIF) was prepared as a fresh 10 mM stock solution in DMSO. Before each experiment the toxins were sonicated. Prior to adding the toxins cytochrome c (0.1 mg ml^{-1}) was added to the recording chamber solution to prevent non-specific peptide binding to containers. The currents were recorded after a 2 min incubation with each blocker.

For the slice culture, pituitary slices from adult male mice were transferred on to the culture plate mesh (Millicell-CM, Millipore, Billerica, MA, USA) and inserted into the plate well (Cellstar, Greiner Bio-One, Kremsmuenster, Austria). Slices were kept in an incubator at 37°C, in 95% humidity and 5% CO_2 in phenol red-free Dulbecco's modified Eagle's medium (DMEM)/F-12 medium (Life Technologies Inc., Grand Island, NY, USA; 100 U penicillin and 100 μg streptomycin per 1 ml of medium; pH 7.2) for 24 h before experimentation. Phenol red-free medium was used due to the weak oestrogenic effect of phenol red observed by Hofland *et al.* (1987) in the anterior pituitary cells. 17β-Oestradiol was prepared as a 3.7 mM stock solution in ethanol. The final ethanol concentration in the medium was less than 0.0001%, thus having no effect on the Ca^{2+} current density (Ritchie, 1993). To test the effect of oestrogen, 1 nM 17β-oestradiol was added to the culturing medium. The control slices for the 17β-oestradiol-treated slices were also cultured for 24 h. This series of experiments were performed in external solution 4 with 5 mM $CaCl_2$.

Results

Currents through VACCs in melanotrophs in fresh pituitary slices

Tissue slice preparation has been used previously to study the electrophysiological properties of the adult rat pituitary (Schneggenburger & Lopez-Barneo, 1992; Schneggenburger & Konnerth, 1992). We expanded the approach by preparing thin slices of an adult as well as newborn mouse pituitary gland. Due to the small size of the gland we had to embed it in low-melting-point agarose. Slices as thin as 40 μm could be made from the agarose cubes, although gross morphology was best preserved in 80 μm slices (Fig. 1*A*).

The whole-cell patch-clamp recordings from the mouse pituitary slices revealed a relatively high density of VACCs not readily seen in fresh dispersed cultures. Indeed, 90% of adult and 89% of newborn melanotrophs showed at least one voltage-activated component of Ba^{2+} currents, which is consistent with previous findings in the rat pituitary (Schneggenburger & Lopez-Barneo, 1992). The resting membrane capacitance, a parameter proportional to the

cell membrane surface area, was significantly larger in newborns (10.6 ± 0.6 pF; $n = 64$) compared to adults (6.4 ± 0.2 pF; $n = 130$; $P < 0.001$).

We have used two different depolarizing voltage protocols to elicit currents through the VACCs (Fig. 1*B*). Inward currents were due to the Ba^{2+} influx through the VACCs since they were completely abolished by 1 mM $CoCl_2$ or removal of extracellular Ba^{2+} (data not shown). Both protocols activated Ba^{2+} currents of comparable amplitudes. Due to the larger membrane surface area the average peak Ba^{2+} current density was smaller in newborn melanotrophs (22.3 ± 2.1 pA pF^{-1}; $n = 34$), but not statistically different from adult melanotrophs (31.3 ± 2.7 pA pF^{-1}; $n = 34$; Fig. 1*C*). In adult cells the amplitude of Ba^{2+} currents slowly decreased with a rate of approximately 1% per minute (Fig. 1*D*), slower than from the reported cultured rat melanotrophs (Cota, 1986; Kocmur-Bobanovic & Zorec, 1996). The initial increase in Ba^{2+} current amplitudes similar to that described in cultured cells (Mansvelder *et al.* 1996; Kitamura *et al.* 1998) was also detected (Fig. 1*D*). During the whole-cell dialysis the cell membrane capacitance steadily decreased at 2% per minute (data not shown), which is consistent with a previous report in cultured cells (Rupnik & Zorec, 1992). The Ba^{2+} current rundown thus merely represented a decrease in the membrane surface area due to endocytosis and not a decrease in the channel density. We made such stable conditions a prerequisite for testing the presence of multiple VACCs on a single cell.

Differential expression of Ba^{2+} currents in newborn and adult melanotrophs

Next, we determined the expression of the different VACCs in the newborn and adult melanotrophs. We routinely applied VACC blockers in the following chronological order with 2 min intervals to establish a steady-state level of the block (Mansvelder & Kits, 2000; for the effect of nifedipine see also Fig. 1*D*: NIF (10 μM), GVIA (1 μM), MVIIC (100 nM) together with TK (100 nM), and $CdCl_2$ (200 μM). Optimal calcium channel blocker concentrations as previously described in the newborn (Beatty *et al.* 1996) and adult melanotrophs (Ciranna *et al.* 1996; Mansvelder *et al.* 1996) were used in our study and no changes in the concentration dependence of inhibition across development in melanotrophs have been reported. Using described voltage protocols we were thus able to isolate L-, N- and P/Q-type VACCs in the adult and newborn melanotrophs. Moreover, we found a significant toxin-resistant Ba^{2+} current in newborn melanotrophs (Fig. 2*A*, *B* and *C*). The majority of the current analysis

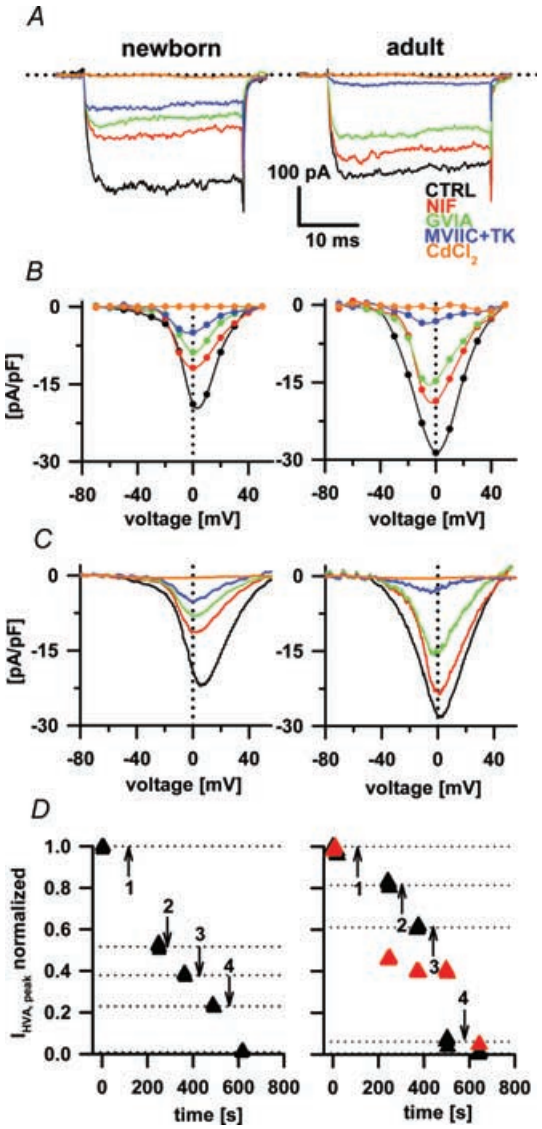

Figure 2. The effects of nifedipine, ω-conotoxin GVIA, ω-conotoxin MVIIC with ω-agatoxin TK and $CdCl_2$ on Ba^{2+} currents

In panels *A*, *B*, *C* and *D* left plots present data from the newborn and right plots from the adult animals. *A*, Ba^{2+} currents were evoked during 30 ms voltage steps from −80 mV to +60 mV. All recordings were obtained after preincubation (2 min) with different VACC blockers as indicated. *B*, current densities from the same cells were plotted to obtain the Ba^{2+} current *I–V* relationship. *C*, the effect of VACC blockers on the Ba^{2+} current *I–V* relationship obtained from 300 ms voltage ramps. *D*, the time course of the effect of nifedipine (1), GVIA (2), MVIIC/TK (3) and $CdCl_2$ (4) on Ba^{2+} currents. LVA currents in adults are shown as red triangles and the HVA are shown as black triangles. Note that current values were normalized to the peak amplitude of both VACC components. Nifedipine blocked about 50% of the LVA component; however, other toxins than Cd^{2+} did not affect the LVA component.

was done by using a 300 ms voltage ramp protocol. The comparison of *I–V* relationships from the steady-state analysis to voltage ramps revealed no quantitative difference in the measured current amplitudes between the two protocols (Figs 1*B* and 2*B* and *C*). This confirmed that the 300 ms voltage ramp protocol is an adequate assay to measure Ba^{2+} current amplitudes over the entire voltage range (Kocmur & Zorec, 1993) and allows a higher number of *I–V* tests per experiment to be performed on a single cell. This approach also enabled us to rapidly assay the action of different channel blockers on HVA channels (Fig. 2*D*).

The averaging of at least five consecutive *I–V* plots in control and test conditions resulted in low noise records, which were used to isolate time profiles of the Ba^{2+} currents through different Ca^{2+} channel types (Fig. 3*A*). The subtraction of the Ba^{2+} current after addition of nifedipine from the current in control conditions revealed both LVA and HVA components of nifedipine-sensitive currents (Fig. 3*A*, right), which is consistent with the previous report (Akaike *et al.* 1989). The LVA component peaked at around −20 mV and the HVA component at around +10 mV. No obvious LVA component was detected in newborn melanotrophs (Fig. 3*A*, left). Melanotrophs lacking LVA were also previously described in rat melanotrophs (Kocmur & Zorec, 1993).

To block the L-type VACCs we applied the maximally effective concentration of nifedipine (10 μM) (Ciranna *et al.* 1996). Nifedipine-sensitive current peak amplitude was attenuated by 25.3 ± 3.2% ($n = 25$) in adult and 46.4 ± 7.4% ($n = 13$); $P < 0.002$) in newborn melanotrophs (Fig. 3*B*).

The further application of GVIA blocked a comparable amount of the HVA current in the adult and newborn melanotrophs, by 27.5 ± 4.8% ($n = 13$) and 23.3 ± 3.1% ($n = 7$), respectively (Fig. 3*B*). A cocktail of MVIIC and TK provided a complete block of P/Q-type VACCs (Ciranna *et al.* 1996). Using this cocktail we were able to block significantly more Ba^{2+} currents in adult melanotrophs (50.2 ± 6.3%, $n = 11$) compared to the newborns (17.3 ± 3.3%, $n = 7$; $P < 0.001$; Fig. 3*B*). The toxin-resistant peak Ba^{2+} current in adult melanotrophs was 3.7 ± 1.9% ($n = 10$). However, the application of all mentioned calcium channel blockers to newborn melanotrophs revealed a relatively large toxin-resistant Ba^{2+} component (13.7 ± 3%, $n = 5$; $P < 0.001$; Fig. 3*B*). The susceptibility of these toxin-resistant currents to a specific R-type channel blocker SNX-482 (50 nM) was also tested (Newcomb *et al.* 1998). SNX-482 and $NiCl_2$ (50 μM) only partially blocked the residual toxin-resistant Ba^{2+} currents (2.5 ± 1.9%, $n = 8$), but they could be totally abolished using $CdCl_2$ (34.6 ± 8.9%, $n = 10$; not shown). It is likely that newborn melanotrophs express a SNX-482-insensitive variant of toxin-resistant currents (Sochivko *et al.* 2003).

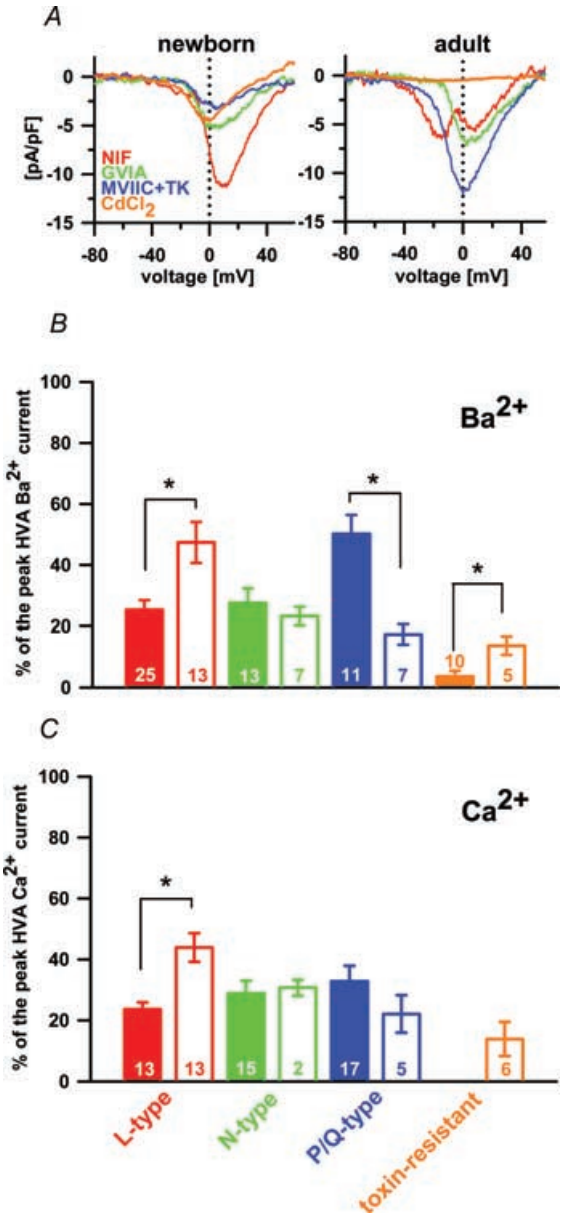

Figure 3. The separation of different VACCs in Ba^{2+} and Ca^{2+}
A, separated Ba^{2+} current densities through L-, N- and P/Q-type VACCs and toxin-resistant channels in newborn (left panel) and adult melanotrophs (right panel). Note the first peak in the nifedipine-sensitive current in adults is the LVA component and second peak the HVA component (red trace). *B*, the contribution of different VACC types to the peak HVA Ba^{2+} current: adult, filled bars; newborn, open bars. *C*, contribution of different VACC types to the peak HVA Ca^{2+} current: adult, filled bars; newborn, open bars. The toxin-resistant current was negligible in adult melanotrophs and was therefore not tested for statistical significance.

Differential expression of Ca^{2+} currents in newborn and adult melanotrophs

Ba^{2+} as a charge carrier did increase the amplitude of currents through the VACCs. However, Ba^{2+} currents only partially supported the secretory activity (not shown) compared to conditions where Ca^{2+} carried the charge. For the analysis of the VACCs directly involved in the development of the endocrine function we therefore replaced Ba^{2+} with Ca^{2+}. Surprisingly, the relative densities of the VACC types in experiments with Ca^{2+} ions did not entirely match the distribution of VACC types in Ba^{2+}-based experiments. This time, nifedipine inhibited 23.0 ± 4.1% (n = 13) of the peak amplitude of the HVA Ca^{2+} current in the adult and 42.0 ± 7.0% (n = 13) in newborn melanotrophs (Fig. 3*C*), which was significantly different ($P < 0.001$). The application of GVIA blocked a comparable amount of the HVA current in the adult and newborn melanotrophs, by 27.0 ± 4.8% (n = 15) and 26.0 ± 3.1% (n = 2), respectively (Fig. 3*C*). Residual currents in adult melanotrophs ran through P/Q-type calcium channels and were thus completely blocked by MVIIC and TK. A comparable degree of blockage was also observed in adult melanotrophs 29.0 ± 6.3% (n = 17) compared to the newborns, where 20.0 ± 3.3% (n = 5) of the current was blocked (Fig. 3*C*). There was no toxin-resistant component in the Ca^{2+} current in adult melanotrophs and there was 13.9 ± 5.6% (n = 6) in newborn melanotrophs (Fig. 3*C*). In adult melanotrophs there seemed to be no dominant type of VACCs when Ca^{2+} currents were studied. However, in newborns the L-type was significantly up-regulated and an additional toxin-resistant current was expressed.

Ca^{2+} channel subtypes responsible for secretory activity in melanotrophs

In a fresh newborn and adult pituitary slice the Ca^{2+} current density sufficed to support depolarization-induced Ca^{2+}-dependent secretory activity (Fig. 4). The $[Ca^{2+}]_i$ transiently increased to several micromolar during the depolarizing train and subsequently returned to the resting activity (Fig. 4*A* and *B*). The time profile of the $[Ca^{2+}]_i$ change was almost identical between the newborn and adult cells. However, a train of depolarizing pulses induced a higher increase in membrane capacitance due to secretory activity in newborn compared to adult melanotrophs (Fig. 4*C*). The capacitance increase was regularly followed by a significantly slower decrease reflecting endocytosis.

The depolarization which induced secretory activity was reported to run down during whole-cell dialysis and in an activity-dependent manner in some endocrine systems (Ämmälä *et al.* 1993). No major rundown in secretory activity was observed during the whole-cell dialysis, when at least a 6 min interval between two depolarization trains was permitted (Fig. 5*A*). The triggered capacitance response was significantly larger in newborn melanotrophs (1067 ± 110 fF, n = 19) compared to the adults (597 ± 44 fF, n = 97; $P < 0.001$; Fig. 5*B*). Nifedipine reduced the average secretory response by 118 ± 27 fF (n = 17) in adult and by 283 ± 50 fF (n = 8) in newborn melanotrophs

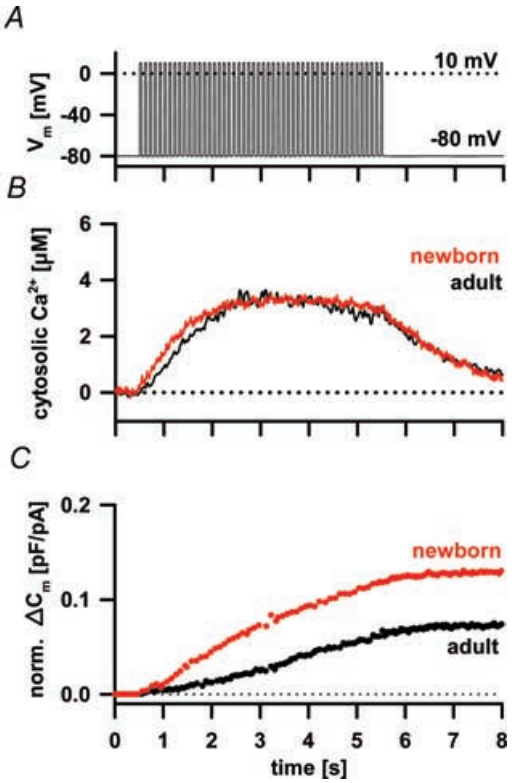

Figure 4. Depolarization induced the increase in the $[Ca^{2+}]_i$ and the secretory activity in newborn and adult melanotrophs
A, changes in $[Ca^{2+}]_i$ were triggered by a train of 50 depolarization pulses (40 ms) from −80 mV to 10 mV and 100 ms interval (*B*) measured with fura-6F. The $[Ca^{2+}]_i$ increased rapidly, reached a plateau at the concentration of several micromolar after 3 s of stimulation and decreased to the resting value after the end of stimulation. Note similar time profile of $[Ca^{2+}]_i$ in newborn (red trace) and adult melanotrophs (black trace). *C*, normalized cumulative membrane capacitance change to the resting membrane capacitance (norm. ΔC_m) did not tightly follow the changes in $[Ca^{2+}]_i$. Norm. ΔC_m increased slower than $[Ca^{2+}]_i$, and persisted despite $[Ca^{2+}]_i$ reaching the maximum. After the end of the stimulation, melanotrophs reached their C_m peak values followed by slow endocytosis for several tens of seconds to reach the steady state level.

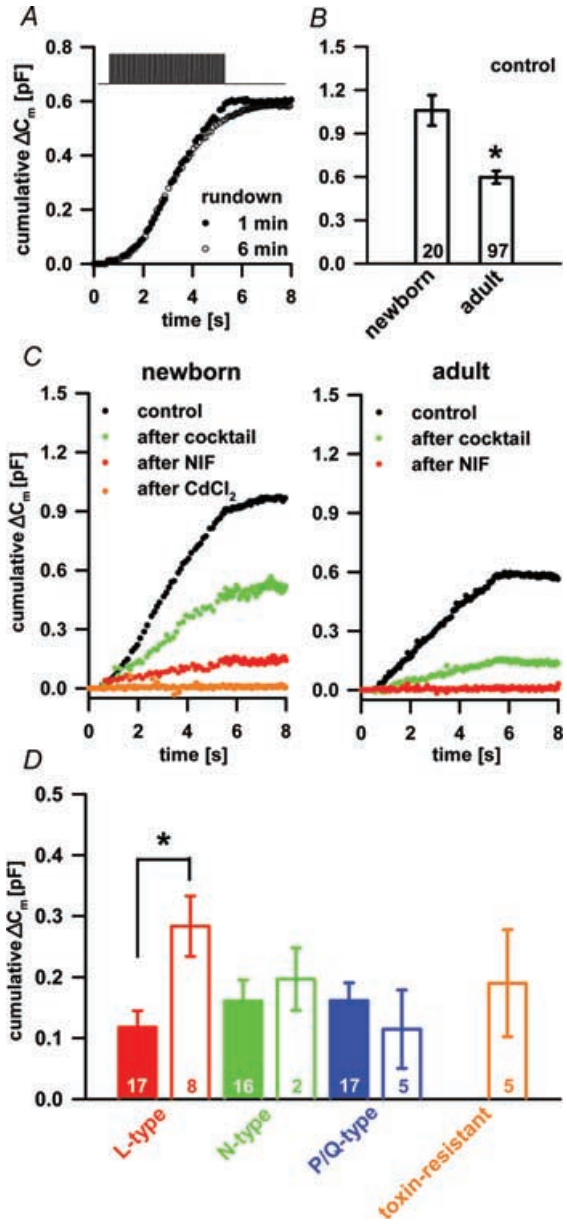

Figure 5. The Ca^{2+}-dependent secretory activity in newborn and adult melanotrophs

A, the rundown of the secretory activity during 6 min of whole-cell dialysis. For details about the voltage protocol used see Fig. 4*A*. *B*, bar graph showing higher C_m increase in control conditions in the newborn compared to the adult melanotrophs. Numbers on the bars represent the number of cells tested. Asterisk shows the statistical difference ($P < 0.001$; Student's *t* test). *C*, typical C_m recordings in newborn (left panel) and adult (right panel) in control conditions (black), after cocktail (composed of GVIA, MVIIC, TK; green), after nifedipine (red) and $CdCl_2$ (orange). *D*, bar graph showing contribution of different VACCs to the total C_m change. The expression of L-type channels was significantly higher in the newborn than adult melanotrophs, whereas other VACCs did not show age-dependent expression. Note also that the toxin-resistant current contributed equally to the capacitance increase just like the L-type channels. Asterisk shows the statistical difference ($P < 0.004$; Student's *t test*).

(Fig. 5*C* and *D*), which was significantly different ($P < 0.004$). The actual percentage inhibition in the capacitance by nifedipine in the newborn was 36.5 ± 4.1% ($n = 8$) and 21.9 ± 2.9% ($n = 17$) in the adult melanotrophs, which was statistically different ($P < 0.01$). The increased secretion in newborn melanotrophs was primarily due to the relative increase of the L-type channel density and the resting membrane capacitance as a parameter of the membrane surface area. The application of GVIA exerted a comparable block of the secretory activity in adult and newborn melanotrophs by 161 ± 34 fF ($n = 16$) and 197 ± 51 fF ($n = 2$), respectively (Fig. 5*C* and *D*). A block of P/Q-type VACCs produced a comparable degree of blockage of the secretory activity in adult melanotrophs (161 ± 29 fF; $n = 17$) and in the newborns (115 ± 64 fF; $n = 5$; Fig. 5*C*). There was no toxin-resistant component in the Ca^{2+}-dependent secretory activity in adult melanotrophs and this component contributed 190 ± 88 fF ($n = 5$) in newborn melanotrophs (Fig. 5*C*). In adult mouse melanotrophs all types of VACCs contributed equally to the secretory activity as reported for cultured rat melanotrophs (Mansvelder & Kits, 2000). However, in newborn melanotrophs the L-type VACCs seemed to be the dominant channel type in supporting the secretory activity, a finding in accord with the reports from adrenal glands of younger animals (Artalejo *et al.* 1994).

Oestrogen-dependent modulation of L-type channels

To trace the source of the differential expression of L-type channels between adult and newborn melanotrophs, we first tested whether it was due to sex hormones. Indeed, nifedipine inhibited 7.4 ± 1.2 pA pF^{-1} of the Ba^{2+} current density in the adult male ($n = 13$), 16.8 ± 3.2 pA pF^{-1} in adult female melanotrophs ($n = 12$) and 15 ± 3.2 pA pF^{-1} in newborn melanotrophs ($n = 12$) ($P < 0.002$; one-way ANOVA; Fig. 6*A*). This represented about 14%, 39% and 46% of the HVA Ba^{2+} current peak amplitude in the adult male, adult female and newborn melanotrophs, respectively (not shown). The expression of N- and P/Q-type VACCs was comparable between the male and female (not shown). The observed significantly higher L-type Ba^{2+} current density in female melanotrophs compared to the males matched with the Ba^{2+} current density in the newborns (Fig. 6*A*). This led us to test the hypothesis that sex hormones, particularly oestrogen, modulate the L-type channels. Oestrogen was previously reported to up-regulate the L-type VACCs in lactotrophs (Cherñavsky *et al.* 1993). Overnight incubation of adult male pituitary slices in 17β-oestradiol (1 nM) significantly increased the peak of the HVA Ca^{2+} current density to 18.6 ± 1.9 pA

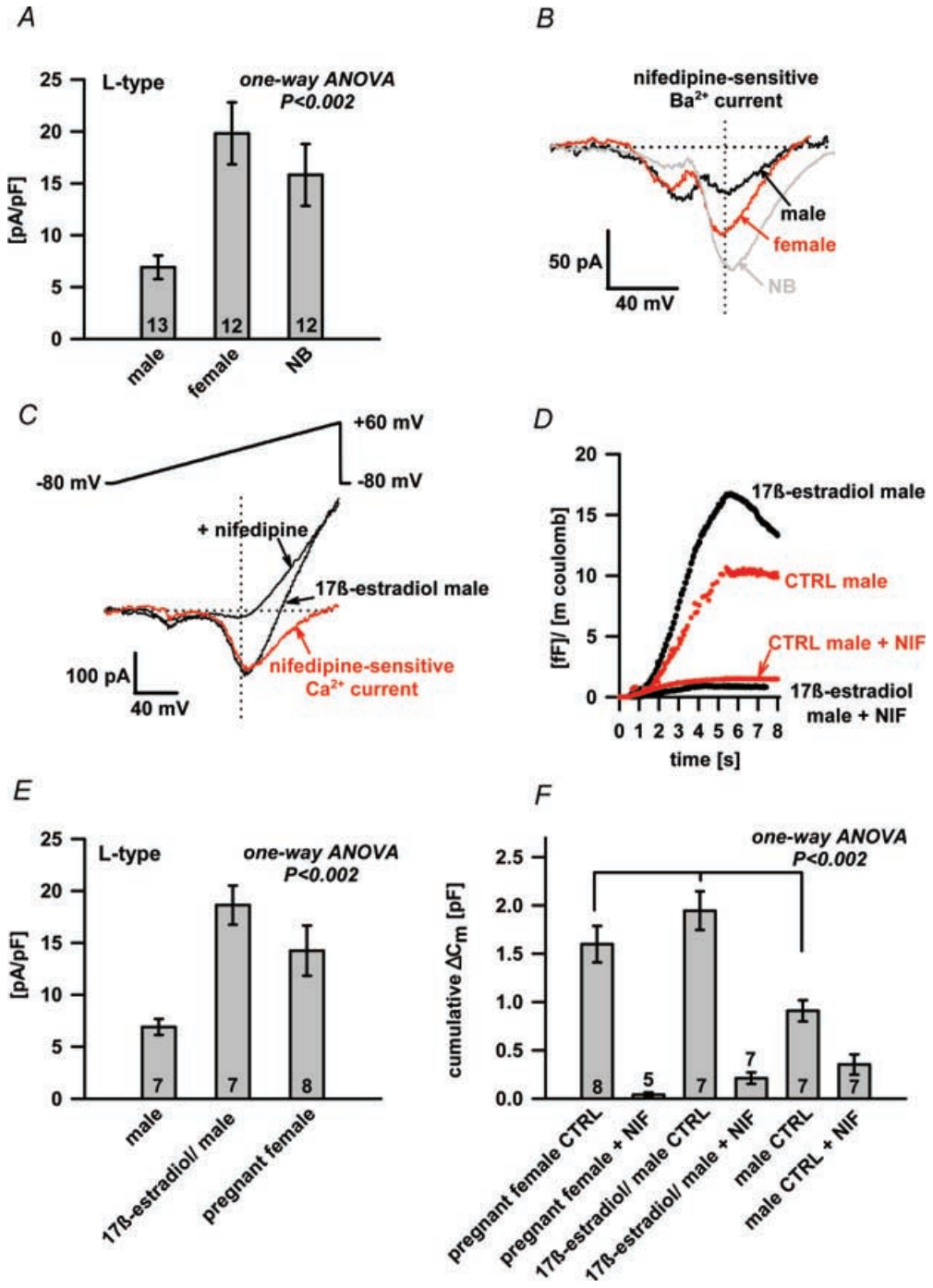

Figure 6. The oestrogen effect on the L-type Ca^{2+} current and C_m changes

A, the difference in nifedipine-sensitive Ba^{2+} current density between adult male, adult female and newborn (NB) melanotrophs. HVA peak Ba^{2+} current amplitudes were statistically different ($P < 0.002$; one-way ANOVA). Numbers on bars represent the number of cells tested. *B*, typical nifedipine-sensitive Ba^{2+} current recordings from the adult male (black trace), adult female (red trace) and newborn (NB) melanotroph (grey trace). Note the comparable LVA component and the different HVA current between adult male, adult female and newborn (NB) melanotrophs. *C*, the representative Ca^{2+} current recording from male melanotrophs incubated 24 h in 1 nM 17β-oestradiol before (arrow) and after nifedipine treatment (arrow). A major part of the Ca^{2+} current amplitude was nifedipine sensitive (red trace). *D*, the representative normalized cumulative membrane capacitance responses to the train of depolarizing pulses from male melanotrophs incubated 24 h in 17β-oestradiol before and after the nifedipine treatment (black traces). Secretory responses of control male melanotrophs only incubated in phenol

pF^{-1} ($n = 7$). In contrast, the Ca^{2+} current density from the control adult male pituitary slices incubated overnight without 17β-oestradiol was 7.3 ± 0.9 pA pF^{-1} (n = 7). Similar up-regulation, 13.7 ± 2.6 pA pF^{-1} ($n = 8$, Fig. 6*E*), was present in melanotrophs of pregnant mice (day 19; $P < 0.002$, one-way ANOVA). Up-regulation was due to the increase of the Ca^{2+} current exclusively through nifedipine-sensitive VACCs (Fig. 6*C*), since these channels represented about 86% of total Ca^{2+} currents in pregnant mice and 84% in 17β-oestradiol-treated male slices, respectively (not shown). This differed significantly from non-treated adult male pituitary slices, in which around 33% of total Ca^{2+} currents were due to the L-type VACCs (not shown). Accordingly, L-type channels were also dominant in triggering the secretory activity in oestrogen-rich pituitaries (Fig. 6*F*). 17β-Oestradiol-treated male pituitary slices and melanotrophs of pregnant mice demonstrated a comparable increase of secretory activity by 1945.6 ± 199.2 fF ($n = 7$) and 1498.7 ± 215.3 fF ($n = 8$), respectively (Fig. 6*F*). This was about 2-fold higher compared to the control male pituitary slices, where the change in the membrane capacitance was 966.1 ± 135.9 fF ($n = 7$; Fig. 6*F*; $P < 0.002$, one-way ANOVA). The application of nifedipine abolished almost completely the secretory response triggered by a train of depolarization pulses (Fig. 6*D*). Melanotrophs from an oestrogen-rich environment, pregnant females and 17β-oestradiol-treated males, also had larger resting membrane capacitances (8.8 ± 0.5 pF, $n = 11$, and 8.0 ± 0.6 pF, $n = 8$, respectively) compared to non-treated adult cells (female: 6.6 ± 0.3 pF, $n = 55$; and male: 6.2 ± 0.2 pF, $n = 75$, both $P < 0.001$).

To test whether oestrogen has a non-genomic effect on L-type Ca^{2+} channels, we perfused the male and female pituitary acute slices with 10 nM 17β-oestradiol for several minutes. Oestrogen concentrations of 10–100 nM are used routinely to investigate rapid oestrogen actions on cells *in vitro* (Kelly & Levin, 2001). No noticeable change in the Ca^{2+} current amplitude or Ca^{2+} channel kinetics was detected during the first 10 min of perfusion (not shown). Thus, it is likely that oestrogen acts on the expression of L-type Ca^{2+} channels at the genomic level and does not influence the kinetic of L-type VACCs.

Discussion

A fresh slice preparation from the pituitary is fast and omits enzymatic treatment and mechanical stress (Schneggenburger & Lopez-Barneo, 1992). Agarose embedding allows the cutting of tiny samples even from the newborns of smaller rodents where cell dispersion for culturing is limiting (Fig. 1*A*). The fresh nature significantly improves the usefulness of the preparation for studying differences between the newborn and adult pituitary cells, particularly the development of their function. The basic electrophysiological characterization of rat melanotrophs in slices has been previously reported (Schneggenburger & Konnerth, 1992). However, the present paper is the first electrophysiological description of the VACCs and their role in the secretory activity using the slice approach in mouse melanotrophs. For the first time we have extended the slicing method to a newborn mouse pituitary, making it a suitable neuroendocrine model system for studying VACCs and hormone secretion at late embryonic and early postnatal stages. The latter knowledge is crucial for assessing the secretory activity in knockout mice missing a key secretory protein and showing a perinatal mortality.

So far, most VACC-related studies have used depolarization pulse protocols in order to separate LVA and HVA components to study the kinetics of the channels. The channel kinetics has not been crucial for our analysis, and the 300 ms voltage ramp protocol turned out to be an adequate way to record currents through VACCs (Kocmur & Zorec, 1993), since we obtained comparable Ba^{2+} and Ca^{2+} current amplitudes and *I–V* relationships. The ramp protocol enabled us to record the currents through different VACCs over the entire voltage range in a very short time, reducing the stress on the measured cell (Fig. 2).

Ba^{2+} and Ca^{2+} currents through VACCs in freshly dispersed adult melanotrophs are small and often too

red-free medium before and after the nifedipine treatment (red traces). Note that cumulative C_m was normalized to the Ca^{2+} influx. *E*, the difference in the nifedipine-sensitive Ca^{2+} current density between male melanotrophs in control conditions, 17β-oestradiol-treated male pituitary slices and pregnant female (day 19). HVA peak Ca^{2+} current amplitudes in males were statistically different ($P < 0.002$; one-way ANOVA). Numbers on bars show the number of cells tested. *F*, the comparison of C_m response in pregnant female, 17β-oestradiol treated male pituitary slices and male melanotrophs in control conditions. C_m responses were statistically different ($P < 0.002$; one-way ANOVA). Numbers on bars show the number of cells tested.

small to support depolarization-induced secretory activity (Cota, 1986; Gomora *et al.* 1996). The limited expression of Ca^{2+} channels has been attributed to dopaminergic innervation that keeps VACC expression low and which has been reversed by specific D2 receptor antagonists (Cota & Hiriart, 1989; Gomora *et al.* 1996). A similar role for serotonin (Ciranna *et al.* 1996) and GABA (Kehl *et al.* 1987; Williams *et al.* 1989) has also been reported. Denervation or the prolonged culturing of dispersed adult melanotrophs in a dopamine-free medium significantly increases currents through the VACCs (Cota, 1986; Gomora *et al.* 1996). On the other hand, currents through the VACCs are large in a cell culture from the preinnervated rat pituitaries and they show no time-dependent up-regulation (Gomora *et al.* 1996). In the dispersed culture of adult mouse melanotrophs we found similar tiny currents and time-dependent up-regulation of the VACCs (not shown). In fresh slices of the newborn mouse pituitary we also found Ba^{2+} and Ca^{2+} currents significantly larger compared to the adults; however, this was associated with a larger cell surface area in newborn melanotrophs (Fig. 1*C*). The overall density of the VACCs did not differ significantly. The reduced membrane surface area in the newborn cell cultures and the reduced density of cultured adult rat melanotrophs previously reported by Gomora *et al.* (1996) could be, at least partially, assigned to cell dispersion.

The VACCs in dispersed culture also show a significant rundown (Cota, 1986), which made testing of several VACC blockers on the same cells difficult. In fresh slices the rundown might merely reflected a constant level of endocytosis due to the high $[Cl^-]_i$ as previously reported (Fig. 1*D*; Rupnik & Zorec, 1992).

Several different combinations of VACCs have been reported to be present in adult rodent melanotrophs. Progressively more VACC subtypes have been described, showing the presence of the L- and N-type (Stack & Surprenant, 1991), the L- and P-type (Williams *et al.* 1993), the L- and P/Q-type (Ciranna *et al.* 1996), and finally the L-, N- and P/Q-type (Mansvelder & Kits, 2000). We confirmed pharmacologically the presence of the L-, P/Q- and N-type in adult mouse melanotrophs. In addition, newborn melanotrophs showed a significant toxin-resistant component, which was insensitive to SNX-482.

As shown in Table 1 at least one part of the differential distribution of the VACCs can be attributed to sex differences. Moreover, using the whole-cell patch-clamp technique we established significantly different relative densities of Ba^{2+} currents comparing newborn and adult melanotrophs. Indeed, the extent of the observed variation was similar to that previously reported for the different species (Cuchillo-Ibanez *et al.* 2002). In newborns L-type channels dominated, while melanotrophs from the adult animals showed a statistically higher density of P/Q-type channels (Fig. 3*B*). A toxin-resistant Ba^{2+} current was present exclusively in newborn melanotrophs. The L-type channel dominance in newborns is consistent with previous findings, whereas P/Q-type was dominant in adult rat melanotrophs (Chronwall *et al.* 1995; Beatty *et al.* 1996). Chronwall *et al.* (1995) described that dopaminergic innervation negatively regulates L-type channel activity in adult melanotrophs. In addition, Beatty *et al.* (1996) showed that P/Q-type VACCs up-regulate with age. The latter report also describes age dependence of the N-type; however, this pattern was not found in our experimental conditions. Moreover, the P/Q-type dominance in our experiments appears only when Ba^{2+} was used as a charge carrier, while in Ca^{2+} based experiments more balanced expression of VACCs was found. This observation can be substantiated even further with the fact that melanotrophs generate bursts of action potential during the secretory phase (Mansvelder & Kits, 2000). While the P/Q-type channel undergoes the Ca^{2+} current-dependent inactivation (Forsythe *et al.* 1998), it is thus likely that the proportion of the P/Q current during bursts or ramp depolarization have been over-estimated when using Ba^{2+} as a charge carrier. In other words, Ca^{2+} experiments reflect more the physiological VACC density contributing to the secretory activity, whereas Ba^{2+} experiments point out only the actual relative current density. We confirmed that VACCs coupled to the secretory activity with equal efficacies, as has been already previously reported (Mansvelder & Kits, 2000). Adult and newborn melanotrophs showed almost an identical $[Ca^{2+}]_i$ time profile during depolarization trains. However, the capacitance response was bigger in the newborn compared to the adult. There are several possible explanations for the observed differences. Firstly, newborn melanotrophs might have more secretory vesicles ready to be released. The increased membrane surface area in newborn cells allows more active membrane surface available for fusion. The relative increase of L-type current density in newborn melanotrophs supports sufficient calcium entry and augments the secretory activity (Fig. 4). Secondly, it is possible that the sensitivity of the release mechanism(s) for Ca^{2+} is increased in the newborn relative to the adult. Thirdly, it is also possible that differences occur in the endocytotic rate between the newborn and the adult. And finally, an additional consideration might be that the capacitance response in melanotrophs from newborn mice does not entirely reflect

neurohormone release, but may involve the fusion of additional vesicle types occurring during postnatal growth and differentiation of melanotrophs. Future experiments on the different mouse models ablated in genes involved in secretory activity should provide the definitive explanation.

Therefore, the observed differences between the newborn and adult melanotrophs in the pattern of VACC expression were probably not due only to the previously described differences in the dopaminergic innervation and the culturing process. The heterogeneity in the L-type current density has been attributed to the effect of oestrogen, while these channels were most apparent in the melanotrophs from the adult female, pregnant, 17β-oestradiol-treated male and newborn mice (Fig. 6*A* and *E*). Under physiological conditions, newborn melanotrophs are under tight control and dominated by the maternal hormonal status. Similarly, female melanotrophs are governed by the oestrus cycle, where oestrogen levels regularly oscillate. However, it is likely that differences between males and females may not always be pronounced, especially after ovulation, when oestrogen levels decrease and become comparable with those in males. On the other hand, simulation of the oestrogen-rich environment within physiological levels can evoke the pregnant female or newborn VACC 'phenotype' in male melanotrophs.

The resting membrane capacitance as a parameter of the membrane surface area was larger in the newborn, pregnant female and 17β-oestradiol-treated male melanotrophs but not in adult female cells compared to male melanotrophs. Oestrogen levels determined in serum plasma from the adult female and adult and fetal male mouse were around 120, 45 and 400 pM, respectively (Nelson *et al.* 1992; Couse *et al.* 1995; vom Saal *et al.* 1997). Measurements of plasma oestrogen levels in the fetal male mice (>400 pM) showed that this concentration is about 60% lower compared to the female fetal mice (vom Saal *et al.* 1997). Thus, we do not expect sex differences in VACCs at this stage. It is likely that oestrogen induced cell growth only in the presence of increased physiological levels of oestrogen (above 120 pM) or when 1 nM 17β-oestradiol was applied (Ritchie, 1993).

The increased expression of L-type channels and the increased membrane surface area do significantly augment the secretory activity. However, in melanotrophs we did not observe facilitation of the VACC activity (not shown). The rapid onset of the 17β-oestradiol effect was not observed during the initial 10 min of the whole-cell dialysis. This suggested that the 17β-oestradiol-induced stimulation of secretion is a genomic effect. Orimo *et al.* (1993) reported that at least 30 min is required for the genomic response to oestrogen to occur. It has been previously reported that oestrogen increases the secretion of α-melanocyte-stimulating hormone (α-MSH) from the intermediate lobe (Ellerkmann *et al.* 1992) with a mechanism similar to that described for lactotrophs and hypothalamic neurones (Dufy *et al.* 1979; Toney *et al.* 1992). The proposed signalling pathway places oestrogen up-stream from dopamine, both acting on the level of c-fos gene expression (Cherñavsky *et al.* 1993). Changes in the HVA Ca^{2+} channel expression have also been observed in the primary melanotroph cultures by long-term incubation with neurotransmitters that influence MSH secretion (Cota & Hiriart, 1989). These studies along with the present observation that oestrogen increases L-type Ca^{2+} channel genomic expression demonstrate that the regulation of ion channel expression in pituitary cells may be a dynamic process and could play an important role in the control of pituitary responsiveness during different physiological states, like the oestrous cycle and pregnancy or embryonic development (Ritchie, 1993).

The toxin-resistant channels found in the newborn melanotrophs seemed to be limited to early postnatal life and were not under regulatory oestrogen control.

Sex differences have been previously reported in Ca^{2+} channel channelopathies (Ashcroft, 2000) as well as susceptibility to certain endocrine disorders. For example, in the pathophysiology of diabetes mellitus the same genetic disorder produces a milder phenotype in females (Hagenfeldt-Johansson *et al.* 2001). The phenomenon is likely to be due to the higher expression of facilitatory L-type VACCs and augmented glucose-induced insulin release associated with elevated plasma oestrogen levels.

From our study, we suggest a general mechanism modulating the endocrine secretion in the presence of oestrogen and particularly higher sensitivity to treatments with L-type channel blockers during high oestrogen physiological states.

References

Akaike N, Kostyuk PG & Osipchuk YV (1989). Dihydropyridine-sensitive low-threshold calcium channels in isolated rat hypothalamic neurones. *J Physiol* **412**, 181–195.

Albillos A, Artalejo AR, Lopez MG, Gandia L, Garcia AG & Carbone E (1994). Calcium channel subtypes in cat chromaffin cells. *J Physiol* **477**, 197–213.

Albillos A, Garcia AG & Gandia L (1993). ω-Agatoxin-IVA-sensitive calcium channels in bovine chromaffin cells. *FEBS Lett* **336**, 259–262.

Ämmälä C, Eliasson L, Bokvist K, Larsson O, Ashcroft FM & Rorsman P (1993). Exocytosis elicited by action potentials and voltage-clamp calcium currents in individual mouse pancreatic B-cells. *J Physiol* **472**, 665–688.

Artalejo CR, Adams ME & Fox AP (1994). Three types of Ca^{2+} channel trigger secretion with different efficacies in chromaffin cells. *Nature* **367**, 72–76.

Ashcroft FM (2000). *Ion Channels and Disease*, 1st edn. Academic Press, London.

Beatty DM, Sands SA, Morris SJ & Chronwall BM (1996). Types and activities of voltage-operated calcium channels change during development of rat pituitary neurointermediate lobe. *Int J Dev Neurosci* **14**, 597–612.

Carter TD & Ogden D (1994). Acetylcholine-stimulated changes of membrane potential and intracellular Ca^{2+} ion concentration recorded in endothelial cells in situ in the isolated rat aorta. *Pflugers Arch* **428**, 476–484.

Cherñavsky AC, Valerani AV & Burdman JA (1993). Haloperidol and oestrogens induce c-myc and c-fos expression in the anterior pituitary gland of the rat. *Neurol Res* **15**, 339–343.

Chronwall BM, Beatty DM, Sharma P & Morris SJ (1995). Dopamine D_2 receptors regulate *in vitro* melanotrope L-type Ca^{2+} channel activity via c-fos. *Endocrinology* **136**, 614–621.

Ciranna L, Feltz P & Schlichter R (1996). Selective inhibition of high voltage-activated L-type and Q-type Ca^{2+} currents by serotonin in rat melanotrophs. *J Physiol* **490**, 595–609.

Cota G (1986). Calcium channel currents in pars intermedia cells of the rat pituitary gland. Kinetic properties and washout during intracellular dialysis. *J General Physiol* **88**, 83–105.

Cota G & Hiriart M (1989). Hormonal and neurotransmitter regulation of Ca channel activity in cultured adenohypophyseal cells. *Soc General Physiol Series* **44**, 143–165.

Cote TE, Eskay RL, Frey EA, Grewe CW, Munemura M, Stoof JC *et al.* (1982). Biochemical and physiological studies of the beta-adrenoceptor and the D-2 dopamine receptor in the intermediate lobe of the rat pituitary gland: a review. *Neuroendocrinology* **35**, 217–224.

Couse JF, Curtis SW, Washburn TF, Lindzey J, Golding TS, Lubahn DB *et al.* (1995). Analysis of transcription and estrogen insensitivity in the female mouse after targeted disruption of the estrogen receptor gene. *Mol Endocrinol* **9**, 1441–1454.

Cuchillo-Ibanez I, Albillos A, Aldea M, Arroyo G, Fuentealba J & Garcia AG (2002). Calcium entry, calcium redistribution, and exocytosis. *Ann N Y Acad Sci* **971**, 108–116.

Douglas WW & Taraskevich PS (1978). Action potentials in gland cells of rat pituitary pars intermedia: inhibition by dopamine, an inhibitor of MSH secretion. *J Physiol* **285**, 171–184.

Douglas WW & Taraskevich PS (1980). Calcium component to action potentials in rat pars intermedia cells. *J Physiol* **309**, 623–630.

Dufy B, Vincent JD, Du Fleury HPP, Gourdji D & Tixier-Vidal A (1979). Dopamine inhibition of action potentials in a prolactin secreting cell line is modulated by oestrogen. *Nature* **282**, 855–857.

Ellerkmann E, Nagy GM & Frawley LS (1992). α-melanocyte-stimulating hormone is a mammotrophic factor released by neurointermediate lobe cells after estrogen treatment. *Endocrinology* **130**, 133–138.

Fass DM, Takimoto K, Mains RE & Levitan ES (1999). Tonic dopamine inhibition of L-type Ca^{2+} channel activity reduces α_{1D} Ca^{2+} channel gene expression. *J Neurosci* **19**, 3345–3352.

Forsythe ID, Tsujimoto T, Barnes-Davies M, Cuttle MF & Takahashi T (1998). Inactivation of presynaptic calcium current contributes to synaptic depression at a fast central synapse. *Neuron* **20**, 797–807.

Gandia L, Albillos A & Garcia AG (1993). Bovine chromaffin cells possess FTX-sensitive calcium channels. *Biochem Biophys Res Commun* **194**, 671–676.

Gandia L, Borges R, Albillos A & Garcia AG (1995). Multiple calcium channel subtypes in isolated rat chromaffin cells. *Pflugers Arch* **430**, 55–63.

Gandia L, Mayorgas I, Michelena P, Cuchillo I, de Pascual R, Abad F *et al.* (1998). Human adrenal chromaffin cell calcium channels: drastic current facilitation in cell clusters, but not in isolated cells. *Pflugers Arch* **436**, 696–704.

Gee KR, Archer EA, Lapham LA, Leonard ME, Zhou ZL, Bingham J *et al.* (2000). New ratiometric fluorescent calcium indicators with moderately attenuated binding affinities. *Bioorg Med Chem Lett* **10**, 1515–1518.

Glassmeier G, Hauber M, Wulfsen I, Weinsberg F, Bauer CK & Schwarz JR (2001). Ca^{2+} channels in clonal rat anterior pituitary cells (GH3/B6). *Pflugers Arch* **442**, 577–587.

Gomora JC, Avila G & Cota G (1996). Ca^{2+} current expression in pituitary melanotrophs of neonatal rats and its regulation by D_2 dopamine receptors. *J Physiol* **492**, 763–773.

Hagenfeldt-Johansson KA, Herrera PL, Wang H, Gjinovci A, Ishihara H & Wollheim CB (2001). β-cell-targeted expression of a dominant-negative hepatocyte nuclear factor-1α induces a maturity-onset diabetes of the young (MODY)3-like phenotype in transgenic mice. *Endocrinology* **142**, 5311–5320.

Hamill OP, Marty A, Neher E, Sakmann B & Sigworth FJ (1981). Improved patch-clamp techniques for high-resolution current recording from cells and cell-free membrane patches. *Pflugers Arch* **391**, 85–100.

Heiman ML & Ben Jonathan N (1982). Rat anterior pituitary dopaminergic receptors are regulated by estradiol and during lactation. *Endocrinology* **111**, 1057–1060.

Hernandez-Guijo JM, de Pascual R, Garcia AG & Gandia L (1998). Separation of calcium channel current components in mouse chromaffin cells superfused with low- and high-barium solutions. *Pflugers Arch* **436**, 75–82.

Hofland LJ, van Koetsveld P, Koper JW, den Holder A & Lamberts SW (1987). Weak estrogenic activity of phenol red in the culture medium: its role in the study of the regulation of prolactin release in vitro. *Mol Cell Endocrinol* **54**, 43–50.

Kehl SJ, Hughes D & McBurney RN (1987). A patch clamp study of gamma-aminobutyric acid (GABA)-induced macroscopic currents in rat melanotrophs in cell culture. *Br J Pharmacol* **92**, 573–585.

Keja JA, Stoof JC & Kits KS (1991). Voltage-activated currents through calcium channels in rat pituitary melanotrophic cells. *Neuroendocrinology* **53**, 349–359.

Kelly MJ & Levin ER (2001). Rapid actions of plasma membrane estrogen receptors. *Trends Endocrinol Metab* **12**, 152–156.

Kitamura N, Ohta T, Ito S & Nakazato Y (1997). Calcium channel subtypes in porcine adrenal chromaffin cells. *Pflugers Arch* **434**, 179–187.

Kitamura N, Ohta T, Ito S & Nakazato Y (1998). Calcium channel current facilitation in porcine adrenal chromaffin cells. *Pflugers Arch* **435**, 781–788.

Kocmur L & Zorec R (1993). A new approach to separation of voltage-activated Ca currents in rat melanotrophs. *Pflugers Arch* **425**, 172–174.

Kocmur-Bobanovic L & Zorec R (1996). Nicardipine enantiomers inhibit calcium and outward currents in rat pars intermedia cells. *Neurosci Lett* **207**, 121–124.

Mains RE & Eipper BA (1979). Synthesis and secretion of corticotropins, melanotropins, and endorphins by rat intermediate pituitary cells. *J Biol Chem* **254**, 7885–7894.

Mansvelder HD & Kits KS (2000). All classes of calcium channel couple with equal efficiency to exocytosis in rat melanotropes, inducing linear stimulus–secretion coupling. *J Physiol* **526**, 327–339.

Mansvelder HD, Stoof JC & Kits KS (1996). Dihydropyridine block of ω-agatoxin IVA- and ω-conotoxin GVIA-sensitive Ca^{2+} channels in rat pituitary melanotropic cells. *Eur J Pharmacol* **311**, 293–304.

Nelson JF, Felicio LS, Osterburg HH & Finch CE (1992). Differential contributions of ovarian and extraovarian factors to age-related reductions in plasma estradiol and progesterone during the estrous cycle of C57BL/6J mice. *Endocrinology* **130**, 805–810.

Newcomb R, Szoke B, Palma A, Wang G, Chen X, Hopkins W *et al.* (1998). Selective peptide antagonist of the class E calcium channel from the venom of the tarantula *Hysterocrates gigas*. *Biochemistry* **37**, 15353–15362.

Nussinovitch I & Kleinhaus AL (1992). Dopamine inhibits voltage-activated calcium channel currents in rat pars intermedia pituitary cells. *Brain Res* **574**, 49–55.

Orimo A, Inoue S, Ikegami A, Hosoi T, Akishita M, Ouchi Y *et al.* (1993). Vascular smooth muscle cells as target for estrogen. *Biochem Biophys Res Commun* **195**, 730–736.

Ritchie AK (1993). Estrogen increases low voltage-activated calcium current density in GH3 anterior pituitary cells. *Endocrinology* **132**, 1621–1629.

Rupnik M & Zorec R (1992). Cytosolic chloride ions stimulate Ca^{2+}-induced exocytosis in melanotrophs. *FEBS Lett* **303**, 221–223.

vom Saal FS, Timms BG, Montano MM, Palanza P, Thayer KA, Nagel SC *et al.* (1997). Prostate enlargement in mice due to fetal exposure to low doses of estradiol or diethylstilbestrol and opposite effects at high doses. *Proc Natl Acad Sci U S A* **94**, 2056–2061.

Sakmann B & Stuart G (1995). Patch-pipette recordings from the soma, dendrites and axon of neurons in brain slices. In *Single Channel Recording*, 2nd edn, ed. Sakmann B & Neher E, pp. 199–211. Plenum Press, New York.

Schneggenburger R & Konnerth A (1992). GABA-mediated synaptic transmission in neuroendocrine cells: a patch-clamp study in a pituitary slice preparation. *Pflugers Arch* **421**, 364–373.

Schneggenburger R & Lopez-Barneo J (1992). Patch-clamp analysis of voltage-gated currents in intermediate lobe cells from rat pituitary thin slices. *Pflugers Arch* **420**, 302–312.

Sochivko D, Chen J, Becker A & Beck H (2003). Blocker-resistant Ca^{2+} currents in rat CA1 hippocampal pyramidal neurons. *Neuroscience* **116**, 629–638.

Stack J & Surprenant A (1991). Dopamine actions on calcium currents, potassium currents and hormone release in rat melanotrophs. *J Physiol* **439**, 37–58.

Toney TW, Pawsat DE, Fleckenstein AE, Lookingland KJ & Moore KE (1992). Evidence that prolactin mediates the stimulatory effects of estrogen on tuberoinfundibular dopamine neurons in female rats. *Neuroendocrinology* **55**, 282–289.

Williams PJ, MacVicar BA & Pittman QJ (1989). Identification of a GABA-activated chloride-mediated synaptic potential in rat pars intermedia. *Brain Res* **483**, 130–134.

Williams PJ, Pittman QJ & MacVicar BA (1993). Blockade by funnel web toxin of a calcium current in the intermediate pituitary of the rat. *Neurosci Lett* **157**, 171–174.

Zorec R, Henigman F, Mason WT & Kordaš M (1991). Electrophysiological study of hormone secretion by single adenohypophyseal cells. *Meth Neuroscience* **4**, 194–210.

Acknowledgements

We would like to thank Marion Niebeling and Heiko Röhse for their excellent technical assistance. We cordially thank Erwin Neher for critical reading of the manuscript. The work was supported by Ministry of Education, Science and Sport of the Republic of Slovenia to S.S and R.Z. (P3521-0381), Marie-Curie training site (QLGA-1999-51322) and Center for Molecular Physiology of the Brain (DFG) to S.S., and Japanese Society for Promotion of Science and Max-Planck-Society to M.R.